Journal of Molecular Structure 1273 (2023) 134292

Contents lists available at ScienceDirect

Journal of Molecular Structure

journal homepage: www.elsevier.com/locate/molstr

Synthesis, crystal structure and selected properties of three new 4-propylanilinium polyoxomolybdates

Marcin Oszajca[a,*], Wojciech Nitek[a], Alicja Rafalska-Łasocha[a], Katarzyna Pamin[b], Jan Połtowicz[b], Wiesław Łasocha[a,b]

[a] Faculty of Chemistry, Jagiellonian University, ul. Gronostajowa 2, 30-387 Krakow, Poland
[b] Jerzy Haber Institute of Catalysis and Surface Chemistry PAS, ul. Niezapominajek 8, 30-239 Krakow, Poland

ARTICLE INFO

Article history:
Received 23 March 2022
Revised 27 September 2022
Accepted 6 October 2022
Available online 7 October 2022

Keywords:
Polyoxomolybdates
Octamolybdates
Pentamolybdates
Single crystal studies
Powder diffraction
Hydrocarbon oxidation catalysts

ABSTRACT

Three new polyoxomolybdates of 4-propylaniline were obtained and characterized by X-ray diffraction based crystal structure solution. Structure of compound **1**: bis(4-propylanilinium) pentamolybdate was studied using powder diffraction data, while compounds **2** (tetrakis(4-propylanilinium) β−octamolybdate hydrate) and **3** (hexakis(4-propylanilinium) diacetato-octamolybdate) were studied by single crystal diffraction methods. Compound **3** belongs to a relatively rare group of Mo(VI) compounds containing acetate (CH_3COO^-) groups directly bonded to the Mo atom. Our results indicate an intriguing instability of some polyoxomolybdate compounds, leading to the formation of carboxylic acid containing structure blocks, when such phases are left over in reaction solutions. Thermal stability and the catalytic activity in the hydrocarbons oxidation reactions were studied for these new compounds.

1. Introduction

Polyoxomolybdates are substantial and exciting group of compounds, presenting a number of possible applications in catalysis (typically redox reactions) [1, 2], corrosion inhibition, sensors, and flame retardants [3–5] to name a few. The subgroup of aminium polyoxomolybdates consists of inorganic polyanions formed by Mo-O_x polyhedra, as well as protonated amines acting as counterions as well as structure directing agents. The polyanions may exhibit different dimensionality (clusters, chains, layers etc.) depending on the reaction conditions including, but not limited to: substrates ratio, pH, temperature, reaction time and the type of cation used [5, 6]. Apart from the ionic interaction, cations usually form hydrogen bonds and the number of amine groups that can potentially bond may be considered an important driving factor in the formation of specific structures. Though the influence of these factors on the resulting polymolybdate phases has been widely recognized, the effects of these factors are far from fully predictable.

Catalytic oxidation of hydrocarbons in the liquid phase [7] is widely used in the chemical industry for the synthesis of important large-scale products (e.g. polyamide) as well as for the production of fine chemicals (e.g. fragrances). The oxidation of cyclohexane to cyclohexanone and cyclohexanol in the presence of molecular oxygen as oxidant is a key stage of the method leading to the formation of polyamides like Nylon-6 or Nylon-66. However, the oxidation of cyclohexane is a continuous challenge for chemists because of the low formation efficiency of the desired products. Therefore, new solutions are sought to enable the improvement of the economic and environmental parameters of the cyclohexane oxidation. In order to discover the best catalytic system cyclooctane was selected for laboratory testing out of three cycloalkanes with the general formula CnH2n, where $n = 5, 6, 8$ [6]. It is the most active model substrate for further catalytic study in the oxidation of cycloalkanes with molecular oxygen, which allows a better comparison of the performance of different tested catalysts.Limonene is a very important intermediate for the production of fine chemicals. It is a nontoxic, biodegradable and recyclable medium, readily available as by-product of the citrus industry, which can be transformed into compounds of very high market value. Oxidation of limonene with molecular oxygen produces both epoxidation (limonene oxide) and allylic oxidation (e.g. carveol, carvone) products [8]. Recently, a lot of attention is directed towards limonene oxidation under environmentally acceptable conditions.

Recently, we synthesized three **4**-**pr**opyl**an**iline (**4PrAn**) based new polyoxomolybdates. The obtained compounds belong to well-known structure types in the case of **1** and **2** (pentamolybdates

* Corresponding author.
E-mail address: marcin.oszajca@uj.edu.pl (M. Oszajca).

https://doi.org/10.1016/j.molstruc.2022.134292

Table 1
The carbon, hydrogen and nitrogen percentages determined for the studied compounds.

Compound	Sum formula	Element percentage (obs/calc)		
		C	H	N
1	$C_{18}H_{28}Mo_5N_2O_{16}$	21.59/21.45	2.791/2.80	2.78/2.78
2	$C_{36}H_{58}Mo_8N_4O_{27}$	25.33/24.76	3.603/3.35	3.26/3.21
3	$C_{58}H_{90}Mo_8N_6O_{30}$	32.62/32.88	3.90/4.28	4.376/3.97

and β-octamolybdates respectively) but in the case of **3** an uncommon form of γ-octamolybdate is formed with two acetate groups incorporated into the polyanion. All of the obtained compounds were tested with regard to their catalytic activity towards oxidation of hydrocarbons as it is well known that the family of polyoxomolybdate compounds tends to be active in these reactions with different oxygen donors [2, 6, 9–13]. As the question of which factors regarding polyoxomolybdate compounds are responsible for the efficacy of such catalysts is still open we suppose that analyzing a group of chemically related polyoxometalate compounds may give some insight into the matter. The role of polyoxomolybdate structures in the liquid-phase cyclooctane and limonene oxidation in the presence of molecular oxygen will be also elucidated.

2. Experimental

2.1. Reagents

Molybdic, glacial acetic and hydrochloric acid were purchased at POCh Gliwice (Poland). 4-propylaniline was obtained from Sigma-Aldrich, all reagents were used without any initial purification.

2.2. Synthesis

Compound 1. 0.015 mol of 4-propylaniline mixed with 0.015 mol HCl and 10 ml of H_2O was added to a boiling solution of 0.01 mol of molybdic acid in 150 ml of water. Mixture was boiled under reflux for 12 hrs. gray precipitate with a pale bluish hue was filtered off, washed with a mixture of water and propanol (1:2 ratio) and dried in air.

Compound 2. 0.01 mol of 4-propylaniline mixed with 50 ml of glacial acetic acid was added to a boiling solution of 0.01 mol of molybdic acid in 150 ml of water. Mixture was boiled under reflux for 2 hrs. Obtained clear solution was left for crystallization. After about 2 hrs white crystals of **2** were formed. Crystals were filtered off and dried.

Compound 3. Some of the crystals of **2** were left over in the reaction solution and after a few days they completely transformed into **3**.

3. Elemental analyses

An elemental analysis was performed with the use of a Vario Micro Cube CHNS microanalyzer. The obtained results are collected in Table 1.

3.1. Single crystal diffraction-based structure solution

Single crystal investigations of **2** and **3** were performed using a Bruker-Nonius Kappa-CCD diffractometer with MoK_aradiation. Structure solution and refinement were carried out with the use of SHELXS, SHELXL and WINGX software [14, 15]. Structures were solved through the application of direct methods. All the non-hydrogen atoms were refined with anisotropic displacement parameters. Hydrogen atoms were located using Fourier methods supported by geometric criteria in the cases of -NH_3 and –CH_3 groups.

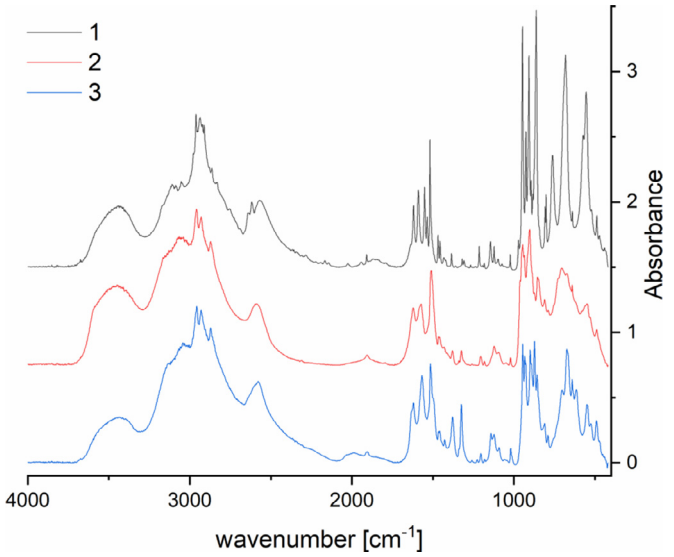

Fig. 1. IR spectra of the studied compounds. Individual spectra are vertically shifted by 0.75 absorbance unit each.

3.2. Powder diffraction studies

Powder diffraction pattern was recorded with the use of PANalytical X'pert PRO MPD diffractometer (CuK_a radiation) equipped with a PIXCEL detector (PSD type). For the determination of cell parameters a measurement in Bragg-Brentano geometry was applied. For the structure determination and refinement stages, the sample was loaded into a borosilicate glass capillary manufactured by Hilgenberg GmbH (diameter of 0.5 mm) and the diffraction pattern was recorded in transmission geometry with the application of a focusing mirror.

The non-ambient powder diffraction experiments were performed on a Philips X'Pert diffractometer (CuKa radiation) equipped with a proportional counter as well as a XRK-900 reaction chamber manufactured by Anton-Paar.

Cell parameters and the space group were determined by PROSZKI package [16]. In the next step the majority of the atoms from the anionic layer were found using EXPO2014 software [17]. Position and orientation of 4-propylaniline was found by a global optimization procedure using FOX [18] program working in parallel tempering mode. Restrained Rietveld refinement was performed in JANA2006 [19].

All the figures presenting structures were prepared using Diamond [20] software.

The quality of the fits obtained in the structure determination is reflected in the R-factor values collected in SI-Table 1, as well as in the case of powder diffraction-based structure determination of **1**, visualized in the Rietveld plot presented in SI-Fig 1. Elevated R-factor values as well as the electron density residuals for **2** and **3** are a result of disorder in the -C_3H_7 substituent of the aminium cations. All of the crystal structures were deposited at the CCDC. The assigned CCDC numbers are collected in SI-Table 1.

3.3. Catalytic tests

3.3.1. Oxidation of cyclooctane in the liquid phase

The catalytic oxidation of cyclooctane selected as a model reaction substrate was performed in a 1 L stainless steel batch reactor at the optimal temperature of 120 °C, under the air pressure of 10

atm and with the molar ratio of cycloalkane to oxygen set at 6.5. In a typical experiment, 0.33 mmol of polymolybdate was introduced into 60 mL of substrate and the was started upon reaching the required reaction conditions. After 6 h of reaction time, the oxidation was stopped by immersing the hot reactor in a cold water bath.

3.3.2. Oxidation of limonene

The catalytic oxidation of limonene was performed in a thermostated glass reactor at the temperature of 80 °C for 6 h at atmospheric pressure. In a typical experiment, 5.8 mmol of catalyst was combined with 10 ml of limonene. The concentration of oxygen was kept constant through the application of a system of valves and a controller which monitored the oxygen levels in the reaction mixture during the reaction.

3.3.3. Catalytic reactions product analysis

The obtained reaction mixtures were analyzed by means of Agilent Technologies 6890 N gas chromatograph equipped with a FID detector and Innowax (30 m) capillary column. GC parameters were quantified in the calibration by using standard samples prior to the analysis. The yields were calculated as the amount of desired product obtained, divided by the theoretical yield.

4. BET measurements

Specific surface areas of the studied compounds were determined by nitrogen adsorption at −196 °C based on BET formalism, using Nova 2000 Quantachrome instrument. Prior to the measurement, the samples were outgassed at 25 °C .

4.1. IR studies

The IR spectra were collected using a Bruker Vertex 70 FTIR spectrometer in the 4000–400 cm^{-1} range with 2cm^{-1} resolution. The samples were prepared by mixing 1 mg of the studied material with 200 mg of KBr and pressing the resulting mixture into pellet form.

5. Results

5.1. Elemental analyses

5.1.1. IR studies

The IR spectra collected for the studied samples are presented in Fig. 1.

5.2. Structures description

Compound **1** is characterized by its layered structure and crystalizes in the monoclinic system (C2/c space group). The asymmetric unit contains three distorted MoO_6 octahedra (Mo-O bonds in the 1.65–2.57 A range), one of which is located in a special position of a twofold axis ((4e) - Wyckoff symbol), as well as a **4PrAn** cation (Fig 2). The polyanion generated by such an arrangement of octahedra is an openwork layer parallel to the (100) plane, constructed through sharing some of the edges and vertices of the polyhedra (SI-Fig1).The $d_{(200)}$ value corresponding to the distance between neighboring anionic layers is ca. 16.81 A (the largest among similar structures studied so far by our group [6]) while the interlayer space is populated by the nearly planar **4PrAn** cations (Fig 3). The cations form moderate to strong N–H**…**O hydrogen bonds with the oxygen atoms from the Mo-O layers which is suggested by the N–O distances lying in the range of 2.531–2.827 A. The individual hydrogen atoms positions were not determined since their electron density contribution was not significant enough. The H-positions could not also be introduced from

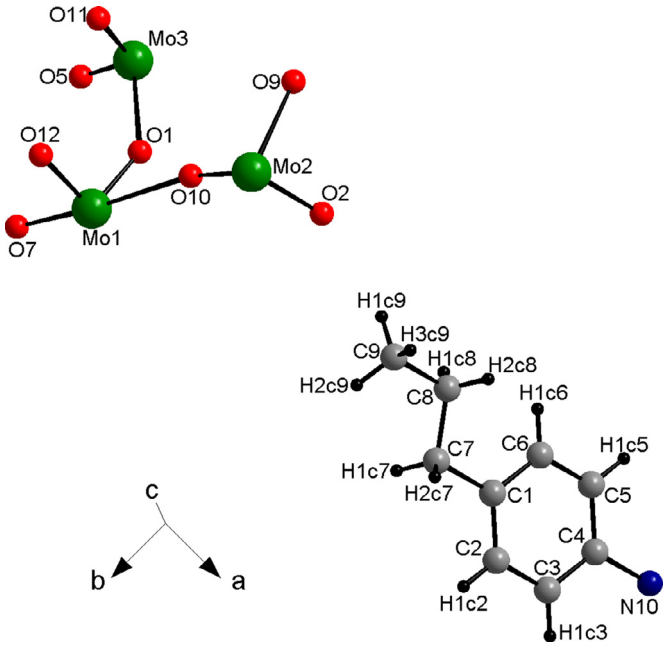

Fig. 2. Asymmetric unit of **1** with the labeling scheme.

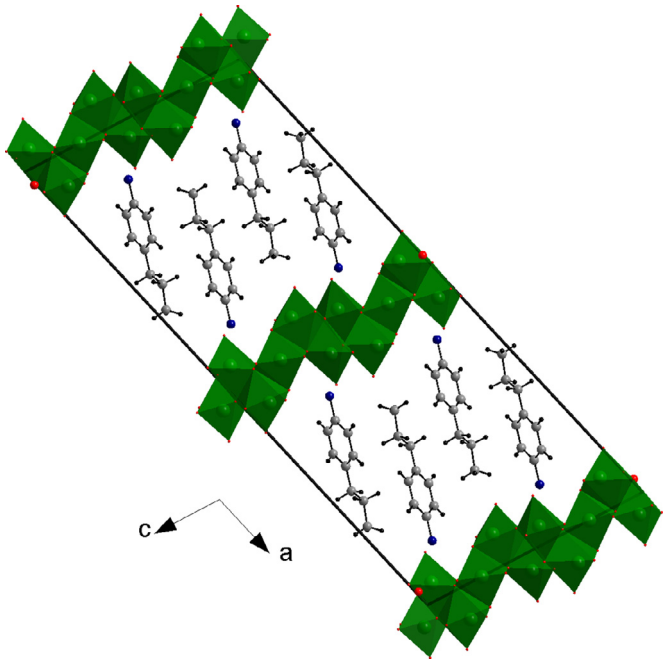

Fig. 3. Packing of **1** showing the alternating arrangement of organic and inorganic layers.

geometrical constraints as with the other hydrogen atoms in the structure since such assumptions would lead to erroneous conclusions regarding the H-bonding system. The relative arrangement of the cations suggests the presence of C–H**…**π bonds between the propyl substituent and the aromatic ring of neighboring aminium moieties.

Compound **2** crystalizes in the triclinic system (P-1 space group) and displays quite a complex structure that required the refinement of 723 parameters and 47 restraints. The asymmetric unit contains two halves of β-octamolybdate anions, four **4PrAn** cations, as well as a single water molecule (Fig 4). Both of the anions are positioned in such a way that their geometric cen-

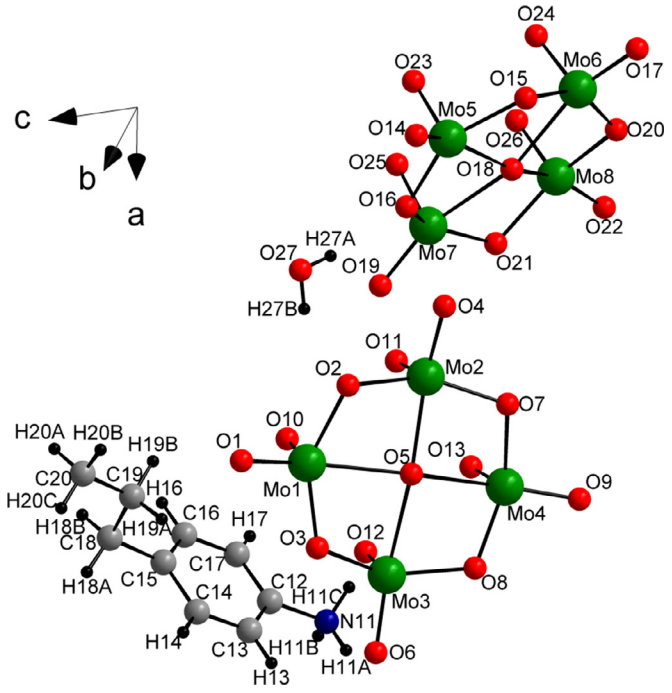

Fig. 4. Asymmetric unit of **2** with the labeling scheme (the 3 missing 4-propylanilinium cations are omitted for clarity; labels for the missing atoms are obtained by adding 10, 20 and 30 to the respective labels in the presented cation).

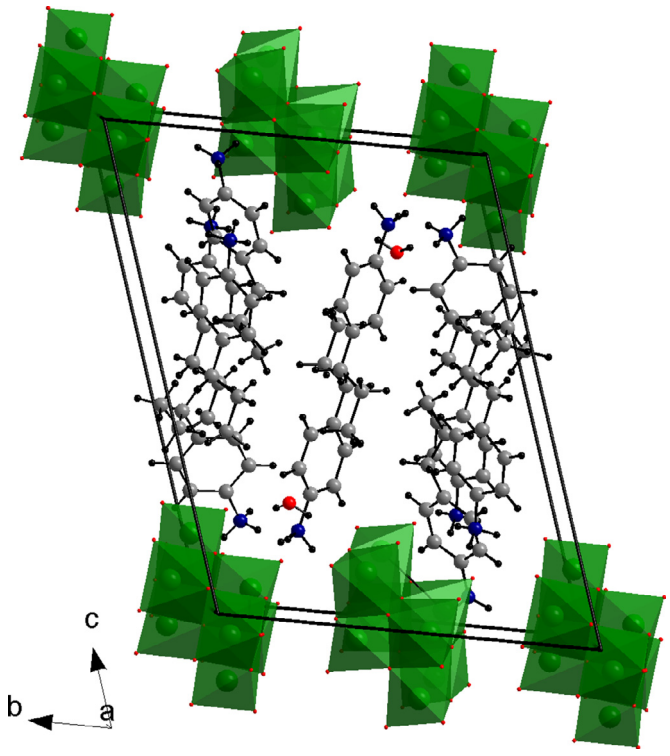

Fig. 5. Unit cell packing for **2**.

ters lie on the inversion centers at ½,0,0 (1d) and ½,½,0 (1e) (Wyckoff positions and corresponding Wyckoff symbols) thus the halves mentioned above are sufficient to describe the complete β-octamolybdate moieties. The anions are composed of 8 distorted MoO_6 octahedra sharing edges with Mo-O bonds in the range of 1.683–2.418 A. Even though there are no direct bonds between individual β-octamolybdate anions, the way they are arranged in the cell allows distinguishing inorganic and organic layers parallel to (001) (Fig 5). The layers alternate and the interlayer distance (defined as the distance between neighboring inorganic layers) is equal to $d_{(001)}$ namely 17.89A. The **4PrAn** cations as well as the water molecules in the structure form H-bonds indirectly joining β-octamolybdate anions with N–O distances in the range of 2.766–3.059 A (2.768 A for amine group-water molecule bond) and the O–O distances of 2.877 A and 2.924 A for water-anion H-bonds. The interactions between the organic cations especially in the -C_3H_7 substituent area are weak, which is a cause for the atomic displacement parameters to be rather large for the terminal carbons in the chain. A second reason would be relative rotational freedom of this group. Three of the four **4PrAn** cations present in the structure of **2** have their alkyl chains twisted out of the aromatic ring plane by approximately 80–100° though the exact values are to be taken with some caution due to the significant displacement values.

Compound **3** crystalizes in the monoclinic system ($P2_1/c$ space group) and the asymmetric unit contains a half of a single centrosymmetric γ-octamolybdate anion as well as three **4PrAn** cations (Fig 6). The complete anion is composed of 8 distorted MoO_6 octahedra, with two of the polyhedra containing oxygen atoms originating from the carboxylic groups of the acetic acid molecules that are bound directly with Mo centers. Even though as in the structure of **2** there are no direct bonds joining individual anions into a larger assembly, the arrangement of Mo-O clusters and the organic cations allows distinguishing separate layers parallel to (100) plane. The interlayer distance corresponding to the separation of neighboring inorganic layers is 20.98 A. Another feature that is similar to **2** is that the atomic displacement parameters for the -C_3H_7 substituent are large, most likely due to rotational freedom in the chain, which is particularly evident when compared with the rest of the structure. The -C_3H_7 chain is also rotated out of plane of the aromatic ring by 80–85. The inorganic and organic parts of the structure are joined via N–H...O hydrogen bonds connecting the amine groups with the oxygen atoms from both the Mo-O cluster as well as from the acetic acids' carboxylic groups (N–O distances between 2.696 A and 3.049 A). Some of these bonds indirectly join individual γ-octamolybdate anions facilitating the formation of the layered structure (Fig 7).

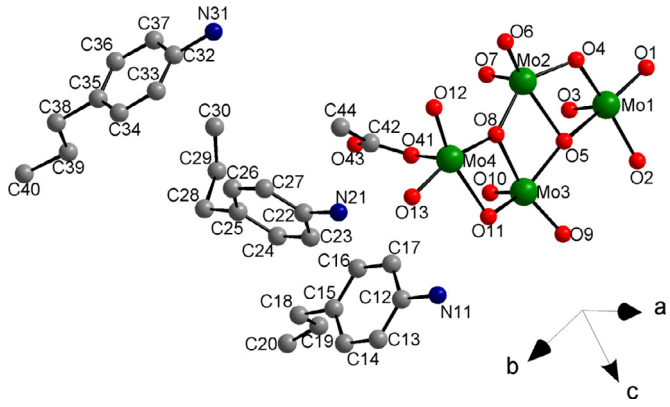

Fig. 6. Asymmetric unit of **3** with the labeling scheme (hydrogen atoms omitted for clarity).

All the details regarding the Mo-O bonding arrangement distances is presented in SI-Table 2.

5.3. Thermal stability test

Thermal decomposition studies using temperature dependent powder X-ray diffraction indicate that in the conditions necessary

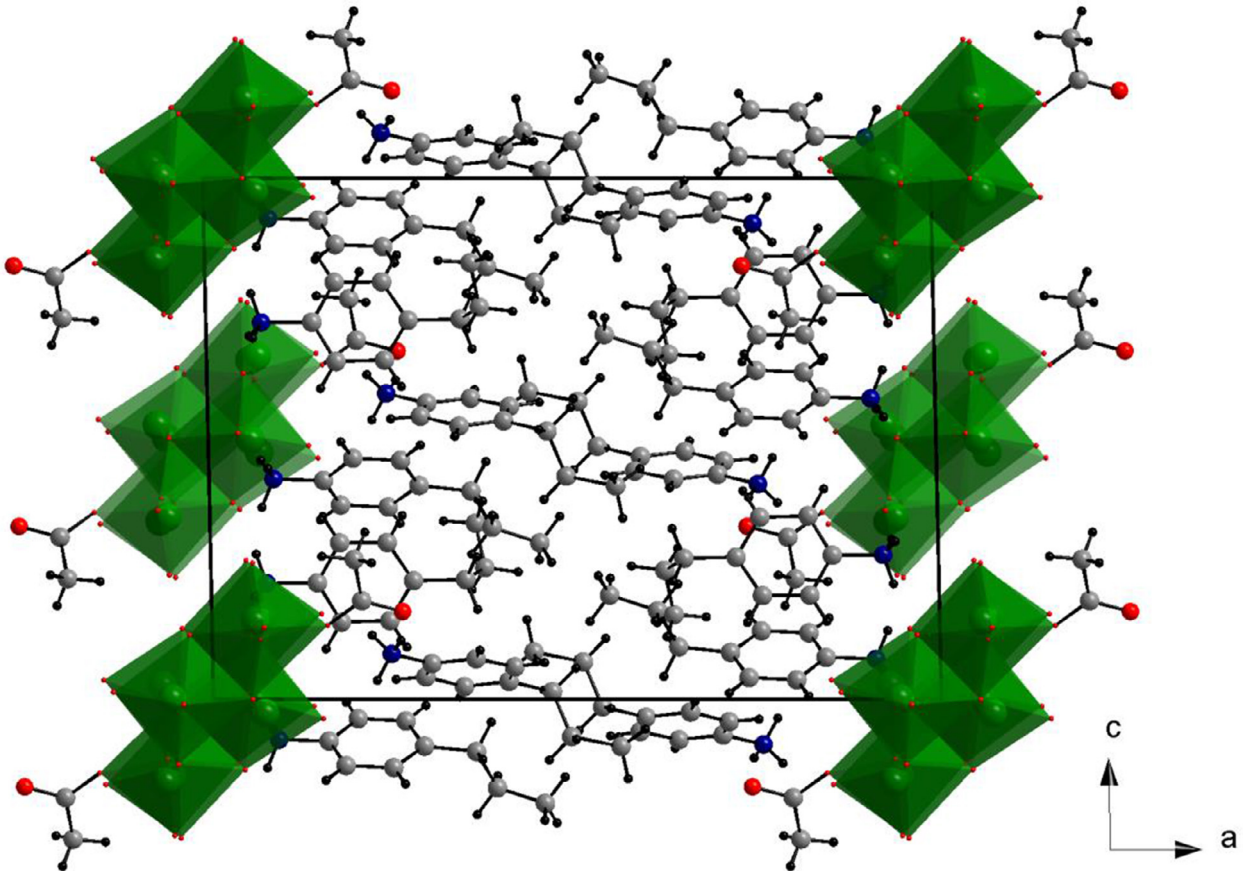

Fig. 7. Unit cell packing for **3**.

Table 2
The results of cyclooctane oxidation.

Compound, formula	Cycloocta-none (A) %	Cycloocta-nol (B) %	Suberic acid (C) %	A+B+C %	A/B	surface area m^2/g
1 $Mo_5O_{16}\{NH_3\text{-}C_6H_4\text{-}C_3H_7\}_2$	29.4	14.9	4.5	48.8	1.97	10.12
2 $Mo_8O_{26}\{NH_3\text{-}C_6H_4\text{-}C_3H_7\}_4\ H_2O$	29.8	17.6	0	47.4	1.69	5.24
3 $Mo_8O_{26}(CH_3COO)_2\{NH_3\text{-}C_6H_4\text{-}C_3H_7\}_6$	28.1	16.9	0	45.0	1.66	3.47

Reaction conditions: Temperature – 120 °C; pressure – 10 atm air; cyclooctane – 60 ml; catalyst amount – 0.33 mmol.

for catalytic oxidation of cyclooctane (conditions described in more detail in the next section), compound **1** is stable, while **2** and **3** decompose around 100 °C. The partial decomposition of **2** observed in ca. 100 °C most likely corresponds to the release of the water molecule present in the structure while for **3** it is probably related with dissociation of acetic acid. The intermediate phase is stable up to 175 °C. All the compounds undergo decomposition coupled with amorphization and at temperatures in the range of 350–400 °C MoO_3 is formed (01–075–0912 [21]). Under the conditions required for the reaction of limonene oxidation (also described in the subsequent section all of the studied compounds are stable. Plots presenting the all the collected diffraction patterns in a function of temperature, are shown in Supporting Information (SI-Fig 3, SI-Fig 4, SI -Fig 5, SI-Fig 6).

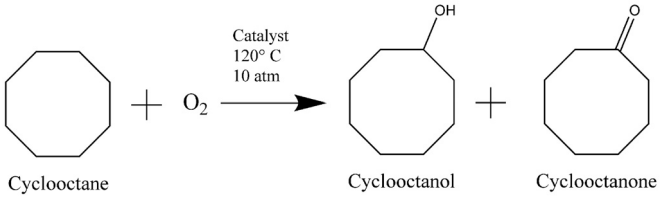

Scheme 1. Scheme of cyclooctane oxidation.

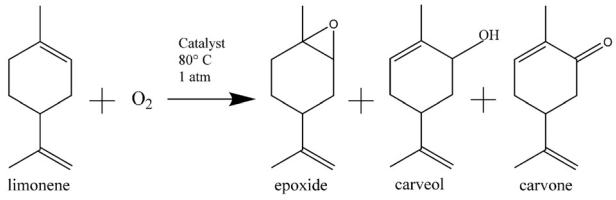

Scheme 2. Scheme of limonene oxidation.

5.4. Catalytic tests

5.4.1. Oxidation of cyclooctane in the liquid phase

Scheme 1 represents the reaction taking place during the catalytic process and lists the expected products. The yields, conversion rates as well as the surface area determined for the studied compounds are collected in Table 2.

5.4.2. Oxidation of limonene

Scheme 2 describes the reaction taking place in the limonene oxidation process and shows the expected reaction products.

The results of the GC analysis are presented in Table 3.

Table 3
Oxidation of limonene.

Catalyst	Conversion of (R+)limonene %	Epoxide %	Carvone %	Carveol %
1 $Mo_5O_{16}\{NH_3\text{-}C_6H_4\text{-}C_3H_7\}_2$	16.1	34. 7	17.9	45.4
2 $Mo_8O_{26}\{NH_3\text{-}C_6H_4\text{-}C_3H_7\}_4H_2O$	4.5	19.9	6.2	49.8.
3 $Mo_8O_{26}(CH_3COO)_2\{NH_3\text{-}C_6H_4\text{-}C_3H_7\}_6$	1.5	12.9	9.2	21.1

Reaction conditions: Temperature – 80 °C; pressure – 1 atm O_2; limonene – 10 ml; catalyst amount – 5.8 mmol.

6. Discussion

The materials synthesized here were obtained in relatively straightforward reactions in which a proper selection of reaction conditions controlled the resulting compound. All of these are formed in acidified aqueous solutions containing appropriate amounts of amine and molybdic acid (H_2MoO_4).

Compound **1** is a typical pentamolybdate that can be compared to the ones previously described in literature, including but not limited to pentamolybdates of 4-methylanilinium and 4-iodoanilinium [22], anilinium [23], 4-bromoanilinium [24], 4-ethylanilinium [6] studied in our group. The openwork Mo-O layers separated by the aminium cations most likely contribute to the specific surface area that is clearly greater for **1** than for the rest of the other compounds described in this manuscript.

Compound **2** belongs to the group of β-octamolybdates [6, 25–27], the most numerously represented isomer in the octamolybdates family. A search of "octamolybdates" keyword in the CSD database returns a significant number of structures and around 60% of them are β-octamolybdates.

Compound **3** is an octamolybdate of the gamma type and is obtained when compound **2** is left in the reaction solution acidified with acetic acid. The structure of two tetragonal Mo-O pyramids located at the opposite vertices of the centrosymetric anions are converted into octahedra by a bond between one of the oxygen atoms of the deprotonated acetic acid molecule and the Mo atom. The molybdenum-oxygen core of the γ-$Mo_8O_{26}(L_2)$ anion is a frequently occurring building block of many complicated polymeric polyoxomolybdates.

Syntheses of compounds **1** and **2** are rather easy, and similar compounds are relatively well known [6, 28]. However, compounds of type **3**, formed by carboxylic acid directly bonding with Mo center from a polyoxomolybdate moiety, are not so frequent with a prevalence of amino acids and small peptides in this group [29–32]. A structure containing the γ-octamolybdate anion with acetic acid ligands occurring in a manner analogous to the one observed here has been published [33]. The crystal structure in question consists of anions found in **3** along with six ammonium cations and 4 water molecules per anion. However, **3** differs through the introduction of larger cations that influence the structure of the material by their characteristic hydrogen bonding arrangement, as well as steric effects introduced by the free rotation of the $-C_3H_7$ substituent of the aromatic ring.

Compound **1** and other pentamolybdates are rather stable in solution as well as in the solid state at elevated temperatures. Compound **2** transforms rather quickly to form **3** if not removed from contact with acetic acid in the reaction solution. Interestingly, even when large excess of acetic acid was applied, no additional carboxylic groups were attached to the octamolybdate anion as a result. This has to be the result of significant stability of the γ-octamolybdate anion with two capping acetate ligands. What is more the transformation of the β-octamolybdate anion into acetate containing form seems to be pretty unique for **3** since analogous experiments performed in similar conditions for 4-ethylanilium β-octamolybdate [6] lead to a pentamolybdate form. Further experiments regarding the conditions in which similar transformations for other aminium β-octamolybdate will be pursed and perhaps this will lead to an explanation of this behavior of **2**. All these observations indicate that 4-propylanilinium polyoxomolybdates are an interesting subject of study even from a purely structural point of view.

The collected IR spectra show high similarities between the obtained phases, which is expected since all the studied materials contain the same organic cations. It is particularly reflected in the high wavenumber region of the spectra due to the presence of the $C–H_{aromatic}$, $C–H_{alkyl}$, and N–H related vibration modes. The increased intensity in the band centered at ca. 3450 for **2** is most likely the result of the O–H vibrations due to the water molecules in the structure, which are not present in other structures. The lower wavenumber region (below 1700 cm^{-1}) is also quite similar, particularly for both octamolybdate spectra (**2** and **3**). In the case of **1**, all the spectral features are significantly sharper and more pronounced. This sharpness of the spectral features is most likely the result of the crystal structure symmetry of **1,** which makes the asymmetric part of the unit cell rather small, especially when compared with the other studied structures. Small number of atoms contributing to the asymmetric part of the cell causes a relative reduction in the number of nonequivalent vibrations in the material, which in turn causes less band overlap. This effect is particularly evident in the 1700–1400 cm^{-1} range, where the $C–C_{aromatic}$ stretching and N–H bending are typically observed. The intensity increase observed for the band at ca. 1565 cm^{-1} in the spectrum of **3** compared to the equivalent part of the spectrum of **2** most likely results from the C–O stretching modes of the acetato- ligand present in **3**.

The region below 1000 cm^{-1} differs significantly between all the collected spectra as it contains major contributions from the Mo-O vibration modes. These modes are strongly dependent on the organization of the polyoxoanion present in the studied material, so it is unsurprising that the vibrations observed for pentamolybdate layers, β-octamolybdate, and γ-octamolybdate clusters are different.

The catalytic studies performed for the studied compounds show that there is observable activity of all catalysts in both reactions (cyclooctene oxidation and limonene oxidation). Thermal stability studies indicate that while **1** remains stable in the cyclooctene oxidation reaction conditions the other compounds affect the reaction outcome as some type of decomposition product instead of the described crystal form. The amorphous character of the decomposed phase in the case of **3** makes it impossible to accurately describe the structure and thus the character of the catalyst in this case. In the case of **2** the decomposition intermediate is most likely a product of dehydration of the starting phase. The presence of suberic acid in the reaction products found for **1** might be a result of higher oxidation achieved due to the diffusion limiting effect of the pentamolybdate layers that hinder the ability of the substrate to vacate the active center.

The A/B proportion from Table 2 represents the ratio of ketone to alcohol (suberic acid was not taken into consideration). The most active catalyst in the cyclooctane oxidation reaction was **1**, which had the total conversion to oxygenates of 48.8%. In this case, the conversion value includes the contribution from the formation of suberic acid along with cyclooctanone and cyclooctanol. The presence of suberic acid in the reaction products was previ-

ously reported for other layered pentamolybdate compounds [6]. **2** demonstrated slightly lower catalytic activity with the total conversion not exceeding 47.4%. The lowest catalytic performance was observed for **3**. In this case, the total yield to alcohol and ketone amounted to 45.0%. The cyclooctanone to cyclooctanol ratio indicates that ketone is the main product of this catalytic reaction. It should be noted that the selectivity to cyclooctanone decreases as the catalytic activity drops. The total observed conversion correlates with the specific surface area for the studied compounds.

The oxidation of limonene was performed under non-solvent conditions in the presence of molecular oxygen acting as oxidant. Usually, limonene can be oxidized to limonene-1,2 oxide in the epoxidation route, which relies on the oxidation of the cyclic ring double bond and to carvone and carveol through the oxidation in the allylic carbon atom. The experiments showed that for all the studied catalysts, oxidation reaction was dominant. The most active catalyst, among the studied polyoxomolybdates, was **1**. In this case, the selectivity towards allylic oxidation products (63.3%) considerably outmatched limonene epoxidation (34.7%). **2** demonstrated moderate catalytic activity, with selectivity to epoxide of 19.9% and to carvone and carveol of 6.2% and 49.8%, respectively. The lowest catalytic activity was exhibited by **3**. The selectivity towards limonene epoxide reached 12.9% and the selectivity to both allylic oxidation products amounted to 30.3%.

As for the cyclooctane case, the catalytic activity in the limonene oxidation reaction correlates with specific surface area since the (*R*+)-limonene conversion reduced significantly between **1, 2**, and **3**.

The activity of **2** and **3** is significantly higher when compared with similar octamolybdate anions-containing phases that we have previously studied (4-methylanilinium and 4-methyl pyridininum based) [6]. The yields observed in cyclooctane oxidation when using **4PrAn** containing compounds are ca. two times higher than for the previous phases. The reason could be the lower thermal stability of the **4PrAn** materials, which leads to the formation of more catalytically active decomposition products (see SI-Fig 4 and SI-Fig 5).

7. Conclusions

7.1. Summary of structural studies

Compound **1** is a layered compound, similar to pentamolybdates of 4-methylaniline, 4-iodoaniline, 4-bromoaniline and aniline. In these compounds there are infinite, layers, composed of MoO_6 octaedra, sharing edges and vertices. The layers have an openwork structure and in the case of **1** are spaced by a distance of 16.81 A.

Compounds **2** and **3** contain anions in the form of isolated clusters. In acetic acid containing solutions β-octamolybdate anions of **2** reorganize significantly and bond with acetate ligands leading to uncommon γ-octamolybdate clusters. This transformation also affects the charge of the form anion as evidenced in the number of propyanilinium cations present in the structure of **3**.

It is worth noting that the compounds similar to the compound **3**, although rare, are known. More common materials containing $Mo_8O_{26}(L)_2$ anions typically have ligands (L) that bond with the Mo atom through a nitrogen atom of an amine or aminoacid molecule.

7.2. Summary of the catalytic investigations

7.2.1. The oxidation of cyclooctane

All compounds are active in the reactions of catalytic oxidation of cyclooctane with molecular oxygen. All compounds exhibit similar catalytic activity and the most active one is compound **1**, which also displays the best selectivity towards ketone. Layered compound **1**, exhibits a behavior similar to the other pentamolybdates [6] and apart from other reaction products, promotes formation of suberic acid.

Activites of both octa-molybdates **2** and **3** in the cyclooctane oxidation are higher than for similar octamolybdates of 4-methylanilinium and 4-methylpyridinium [6]. This might be a result of thermal decomposition of the catalysts, which makes the decomposition products the species actually participating in the catalyzed reactions.

7.2.2. Limonene oxidation

Similarly to the cyclooctane oxidation the most active catalyst of the studied reaction is compound **1**. It can be related to its layered structure and higher specific surface area.

Declaration of Competing Interest

The authors declare that they have no known competing financial interests or personal relationships that could have appeared to influence the work reported in this paper.

CRediT authorship contribution statement

Marcin Oszajca: Conceptualization, Investigation, Writing – original draft, Writing – review & editing, Visualization, Funding acquisition. **Wojciech Nitek:** Investigation, Validation. **Alicja Rafalska-Łasocha:** Investigation. **Katarzyna Pamin:** Investigation, Visualization, Writing – review & editing. **Jan Połtowicz:** Writing – original draft, Writing – review & editing, Resources. **Wiesław Łasocha:** Conceptualization, Investigation, Writing – original draft, Writing – review & editing.

Data Availability

Data will be made available on request.

Acknowledgements

None.

Funding

This work was supported by National Science centre, Poland [grant number 2017/26/D/ST5/01173].

Supplementary materials

Supplementary material associated with this article can be found, in the online version, at doi:10.1016/j.molstruc.2022.134292.

References

[1] K.A. Joergensen, Transition-metal-catalyzed epoxidations, Chem. Rev. 89 (3) (1989) 431–458, doi:10.1021/cr00093a001.
[2] B. Griffe, G. Agrifoglio, J.L. Brito, F. Ruette, Theoretical study of dimeric dioxo-μ-oxo and oxo-bis (μ-oxo) of molybdenum complexes used in catalytic oxidations reactions, Catal. Today 107–108 (2005) 388–396, doi:10.1016/J.CATTOD.2005.07.162.
[3] Ullmann's Encyclopedia of Industrial Chemistry, 6th ed., Wiley-VCH, 2000.
[4] M.T. Pope, A. Müller, polyoxometalate chemistry: an old field with new dimensions in several disciplines, Angew. Chemie Int. Ed. Engl. 30 (1) (1991) 34–48, doi:10.1002/anie.199100341.
[5] M. Cindrić, Z. Veksli, B. Kamenar, Polyoxomolybdates and polyoxomolybdovanadates – from structure to functions : recent results, Croat. Chim. Acta 82 (2) (2009) 345–362.
[6] A. Szymańska, W. Nitek, M. Oszajca, W. Łasocha, K. Pamin, J. Połtowicz, molybdenum complexes as catalysts for the oxidation of cycloalkanes with molecular oxygen, Catal. Lett. 146 (5) (2016) 998–1010, doi:10.1007/s10562-016-1716-7.

[7] U. Schuchardt, R. Pereira, M. Rufo, Iron(III) and copper(II) catalysed cyclohexane oxidation by molecular oxygen in the presence of tert-butyl hydroperoxide, J. Mol. Catal. A 135 (3) (1998) 257–262, doi:10.1016/S1381-1169(97)00314-2.
[8] P.A. Robles-Dutenhefner, M.J. Da Silva, L.S. Sales, E.M.B. Sousa, E.V. Gusevskaya, Solvent-free liquid-phase autoxidation of monoterpenes catalyzed by sol–gel Co/SiO2, J. Mol. Catal. A 217 (1–2) (2004) 139–144, doi:10.1016/J.MOLCATA.2004.03.007.
[9] T.R. Amarante, P. Neves, F.A.A.A. Paz, A.A. Valente, M. Pillinger, I.S. Gonçalves, Investigation of a dichlorodioxomolybdenum(vi)-pyrazolylpyridine complex and a hybrid derivative as catalysts in olefin epoxidation, Dalt. Trans. 43 (16) (2014) 6059–6069, doi:10.1039/c3dt52981a.
[10] C.J. Carrasco, F. Montilla, E. Álvarez, M. Herbert, A. Galindo, Molybdenum-catalysed oxidation of cyclohexene with hydrogen peroxide in the presence of alcohols and X-ray structures of octamolybdate [C 4mim]4[Mo8O26] and tetraperoxodimolybdate [Htmpy]2[{MoO(O2)2} 2(μ-O)] complexes, Polyhedron 54 (2013) 123–130, doi:10.1016/j.poly.2013.02.027.
[11] B. Bożek, et al., Simple hybrids based on Mo or w oxides and diamines: structure determination and catalytic properties, Catal. Lett. 150 (3) (2020) 713–727, doi:10.1007/S10562-019-02935-Z/TABLES/4.
[12] C.C.L. Pereira, et al., A highly efficient dioxo(μ-oxo)molybdenum(VI) dimer catalyst for olefin epoxidation, Inorg. Chem. 46 (21) (2007) 8508–8510, doi:10.1021/ic701746r.
[13] J. Pisk, D. Agustin, V. Vrdoljak, R. Poli, Epoxidation processes by pyridoxal dioxomolybdenum(VI) (pre)catalysts without organic solvent, Adv. Synth. Catal. 353 (16) (2011) 2910–2914, doi:10.1002/adsc.201100439.
[14] G.M. Sheldrick, A short history of SHELX, Acta Crystallogr. Sect. A 64 (1) (2008) 112–122, doi:10.1107/S0108767307043930.
[15] L.J. Farrugia, WinGX and ORTEP for windows: an update, J. Appl. Crystallogr. 45 (2012) 849–854, doi:10.1107/S0021889812029111.
[16] W. Lasocha, K. Lewinski, PROSZKI - a system of programs for powder diffraction data analysis, J. Appl. Crystallogr. 27 (3) (1994) 437–438, doi:10.1107/S002188989400066X.
[17] A. Altomare, et al., EXPO2013: a kit of tools for phasing crystal structures from powder data, J. Appl. Crystallogr. 46 (4) (2013) 1231–1235, doi:10.1107/S0021889813013113.
[18] V. Favre-Nicolin, R. Černý, FOX, 'free objects for crystallography: a modular approach to ab initio structure determination from powder diffraction, J. Appl. Crystallogr. 35 (6) (2002) 734–743, doi:10.1107/S0021889802015236.
[19] V. Petříček, M. Dušek, L. Palatinus, Crystallographic computing system JANA2006: general features, Zeitschrift für Krist. - Cryst. Mater. 229 (5) (2014) 345–352, doi:10.1515/zkri-2014-1737.
[20] W.T. Pennington, DIAMOND - Visual crystal structure information system, J. Appl. Crystallogr. 32 (5) (1999) 1028–1029, doi:10.1107/S0021889899011486.
[21] S. Gates-Rector, T. Blanton, The powder diffraction file: a quality materials characterization database, Powder Diffr. 34 (4) (2019) 352–360, doi:10.1017/S0885715619000812.
[22] M. Oszajca, Ł. Smrčok, W. Łasocha, Bis(4-methylanilinium) and bis(4-iodoanilinium) pentamolybdates from laboratory X-ray powder data and total energy minimization, Acta Crystallogr. Sect. C 69 (11) (2013) 1367–1372, doi:10.1107/S010827011302845X.
[23] W. Łasocha, H. Schenk, Crystal structure of anilinium pentamolybdate from powder diffraction Data. The solution of the crystal structure by direct methods package {\it POWSIM}, J. Appl. Crystallogr. 30 (6) (1997) 909–913, doi:10.1107/S0021889897003105.
[24] W. Lasocha, M. Grzywa, M. Oszajca, Molybdates of p-bromoanilinium – synthesis and crystal structure of new catalytic materials, Zeitschrift für Krist. Suppl. 2009 (30) (2009) 387–394, doi:10.1524/zksu.2009.0057.
[25] J.M. Gutiérrez-Zorrilla, T. Yamase, M. Sugeta, Tetrakis(isopropylammonium) β-octamolybdate(VI, Acta Crystallogr. Sect. C 50 (2) (1994), doi:10.1107/s0108270193007371.
[26] W.J. Kroenke, J.P. Fackler, A.M. Mazany, Structure and bonding of melaminium β-octamolybdate, Inorg. Chem. 22 (17) (1983), doi:10.1021/ic00159a015.
[27] W. Xin, X. Xue-Xiang, W. Qui-Ying, Z. Ying-Li, Study of the transformation of alpha- and beta-octamolybdate; crystal structure of bis(triethylammonium)bis(tetrabutylammonium)beta-octamolybdate dihydrate, Polyhedron 11 (12) (1992) 1423–1427, doi:10.1016/S0277-5387(00)83134-4.
[28] J. Gu, X. Jiang, Z. Su, Z. Zhao, B. Zhou, Self-assembly of γ-octamolybdate-based frameworks decorated by 1,3-bis(4-pyridyl)propane through covalent bond, Inorganica Chim. Acta 400 (2013) 210–214, doi:10.1016/J.ICA.2013.02.036.
[29] E. Cartuyvels, K. Van Hecke, L. Van Meervelt, C. Görller-Walrand, T.N. Parac-Vogt, Structural characterization and reactivity of γ-octamolybdate functionalized by proline, J. Inorg. Biochem. 102 (8) (2008) 1589–1598, doi:10.1016/J.JINORGBIO.2008.02.005.
[30] Q.L. Chen, W. Huang, M.L. Chen, J. Lin, Z.X. Cao, Z.H. Zhou, Transformations and reductions of γ-octamolybdates with their monomeric and dimeric amino polycarboxylates, RSC Adv. 4 (50) (2014), doi:10.1039/c4ra03125c.
[31] M. Inoue, T. Yamase, synthesis and crystal structures of γ -type octamolybdates coordinated by chiral lysines, Bull. Chem. Soc. Jpn. 68 (11) (1995), doi:10.1246/bcsj.68.3055.
[32] T. Yamase, M. Inoue, H. Naruke, K. Fukaya, X-ray structural characterization of molybdate-tripeptide complex, [Mo4O12(glycylglycylglycine)2] · 9H2O, Chem. Lett. (7) (1999), doi:10.1246/cl.1999.563.
[33] Z. Xiao, Y. Wei, L. Xu, Y. Wang, The crystal structure of hexaammonium diacetyl-octa-molybdate tetrahydrate, Cryst. Res. Technol. 41 (6) (2006) 595–599, doi:10.1002/crat.200510631.